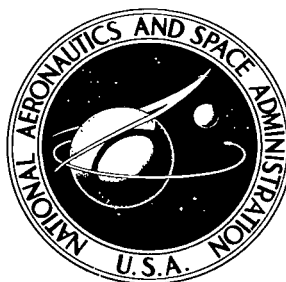


NASA TECHNICAL NOTE

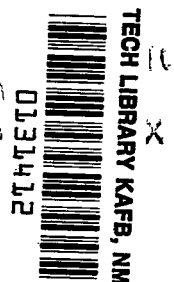


NASA TN D-4497

c.1

NASA TN D-4497

LOAN COPY:
AFWL (1)
KIRTLAND A



DESIGN AND PERFORMANCE OF FLUERIC ANALOG-TO-PULSE-FREQUENCY CONVERTER

by Miles O. Dustin

Lewis Research Center

Cleveland, Ohio

NATIONAL AERONAUTICS AND SPACE ADMINISTRATION • WASHINGTON, D. C. • APRIL 1968





DESIGN AND PERFORMANCE OF FLUERIC ANALOG-
TO-PULSE-FREQUENCY CONVERTER

By Miles O. Dustin

Lewis Research Center
Cleveland, Ohio

NATIONAL AERONAUTICS AND SPACE ADMINISTRATION

For sale by the Clearinghouse for Federal Scientific and Technical Information
Springfield, Virginia 22151 - CFSTI price \$3.00

DESIGN AND PERFORMANCE OF FLUERIC ANALOG- TO-PULSE-FREQUENCY CONVERTER

by Miles O. Dustin
Lewis Research Center

SUMMARY

A flueric circuit which converts an analog pressure signal to pulse frequency is described, and design considerations are discussed. The performance characteristics of a breadboard model are also included. The breadboard model was constructed of commercial flueric amplifiers and one specially developed amplifier.

The circuit uses a three-amplifier, flueric oscillator having a pulsed output whose frequency is a function of input pressure level. The frequency of the oscillator varies continuously from 0 to 180 pulses per second when the input pressure changes from 5.2 psig (36×10^3 N/m² gage) to 3.1 psig (21×10^3 N/m² gage). The complete converter system will operate from 0 to 160 pulses per second when the input pressure to the converter is varied over a range of 2 psi (13.8×10^3 N/m²). The converter system has flat saturation characteristics. The oscillator circuit will recover from a step change in input pressure within one output pulse. The flueric amplifiers use supply pressures of 20 psig (138×10^3 N/m² gage) or less.

The analog-to-pulse-frequency converter will be used to drive a pneumatic stepping actuator system developed for positioning nuclear reactor control drums.

INTRODUCTION

In locations close to a nuclear rocket engine the nuclear radiation level is higher than the tolerance level of most electronic circuit elements. Flueric devices can be constructed of nuclear radiation resistant materials. These devices require no lubrication and can use the engine propellant for the power supply source. Their operation appears to be inherently radiation insensitive. Therefore, they are being considered for control circuits which must be located near the engine.

A pneumatic reactor control drum actuator system is reported in reference 1. A brief description of this actuator system is included in appendix B. (Symbols are defined in appendix A.) To advance the actuator, pulses are supplied to the actuator system; each pulse advances the actuator 0.25° of rotation.

If the actuator system is used in an analog control system, a conversion from an input pressure to pulses proportional to that pressure is required. This report describes the design and performance of an analog-to-pulse-frequency converter which is intended to fulfill this function.

DESIGN OF CONVERTER

Circuit Description and Design Considerations

The functional requirement of the analog-to-pulse-frequency converter circuit is to receive an analog pressure signal and deliver output pulses to a load similar to the actuator system described in appendix B. The frequency of the output pulses is proportional to the deviation of the input pressure from a null value. As shown in figure 1, the null value is set midway in the normal operating range of the input pressure signal. At this value of input pressure, the output pulse frequency is zero. When the input pressure is increased above this value, the output pulse frequency increases and appears at the forward pulse output. As the input pressure decreases from the null value, the output frequency also increases but appears at the backward pulse output. The circuit saturates at a maximum frequency in either the forward or backward direction and remains at that maximum frequency for input pressures greater or less than their normal range.

The maximum frequency was selected as 160 pulses per second. This value is the maximum frequency at which the actuator system of appendix B can satisfactorily operate. The input pressure range is arbitrary and can be selected to be compatible with other elements of a control system.

The analog-to-pulse-frequency converter circuit is made up of three subcircuits, as illustrated in the block diagram of figure 2:

- (1) Oscillator circuit
- (2) Conditioning circuit
- (3) Output selector circuit

Oscillator circuit. - Several oscillators have been developed to convert a pressure signal to an oscillatory output proportional to the input pressure signal. These are reported in references 2 and 3. None of these designs could be used in the analog-to-pulse-frequency converter because in each case the output frequency would not go uniformly to 0 pulses per second.

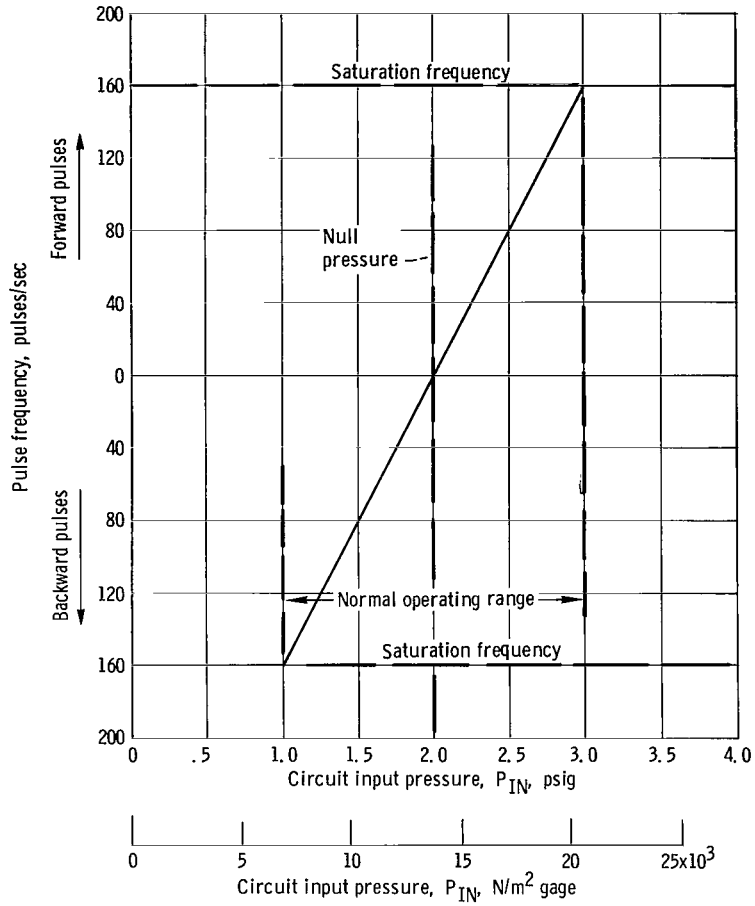


Figure 1. - Desired analog-to-pulse-frequency converter steady-state characteristics.

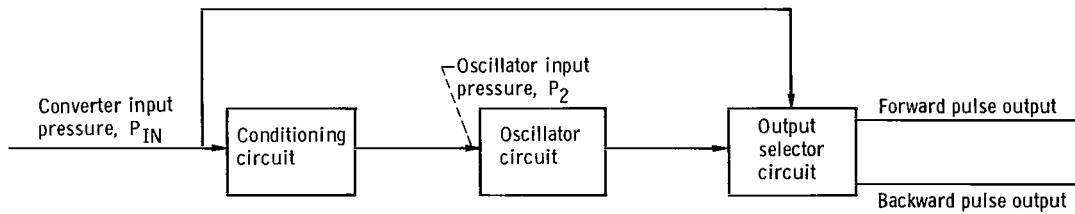
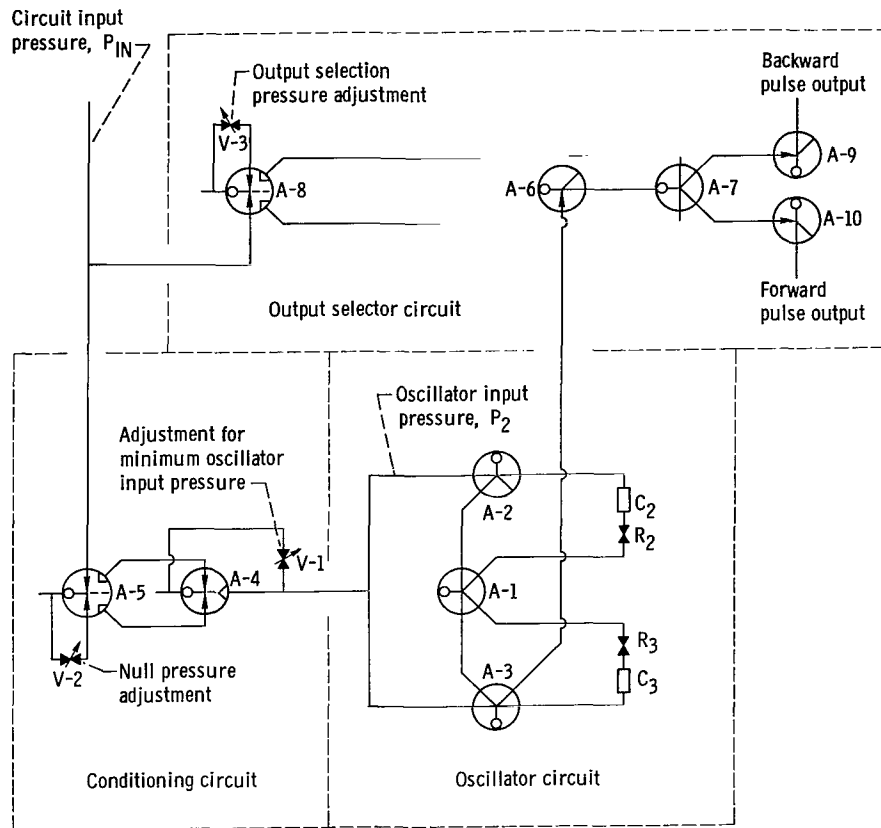


Figure 2. - Analog-to-pulse-frequency converter block diagram.



CD-9527

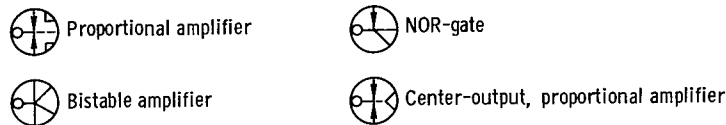


Figure 3. - Schematic diagram of analog-to-pulse-frequency converter.

The oscillator circuit, shown in figure 3, is composed of three bistable amplifiers with R-C time lags in the feedback paths. Amplifier A-1 outputs are connected through resistances and volumes to the control ports of two other amplifiers, A-2 and A-3. One output of each amplifier A-2 and A-3 is then connected to the control ports of amplifier A-1. The input pressure P_2 to the oscillator circuit is connected to both the remaining control ports of amplifiers A-2 and A-3.

To follow the sequence of operation of the oscillator circuit, assume that the output of amplifier A-1 is switched to resistance R_2 . The pressure in volume C_2 rises in a manner approximating a first-order time constant system. When the pressure in volume C_2 is slightly higher than the oscillator input pressure P_2 , amplifier A-2 will switch to the control port of amplifier A-1. This will switch amplifier A-1 to resistance R_3 . As the pressure in volume C_2 drops below the oscillator input pressure

P_2 , amplifier A-2 will switch from the control port of amplifier A-1. However, since amplifier A-1 is bistable, its output will remain switched to R_3 . Similarly, the pressure in volume C_3 rises until it is slightly higher than the oscillator input pressure P_2 , at which time amplifier A-3 switches to the control port of amplifier A-1. Amplifier A-1 then switches to R_2 . When the pressure in C_3 drops below the oscillator input pressure P_2 , amplifier A-3 switches from the control port of amplifier A-1. This completes one cycle.

As the input pressure P_2 increases, more time is required for the volume pressures to exceed P_2 . This increasing time decreases the pulse frequency. The frequency becomes zero when the input pressure P_2 equals the maximum obtainable volume pressure. A plot of calculated output pulse frequency as a function of input pressure for the oscillator circuit is shown in figure 4. The method for determining the calculated curve and the assumptions used are presented in appendix C.

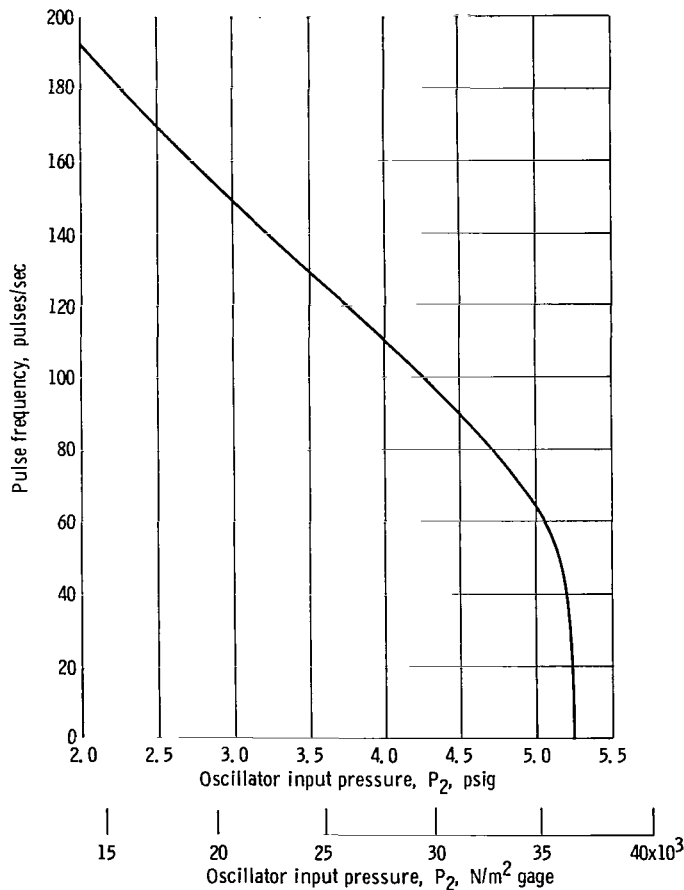


Figure 4. - Calculated oscillator-circuit steady-state characteristics.

Conditioning circuit. - The conditioning circuit is shown schematically in figure 3. The circuit is required to provide an input to the oscillator circuit that is a maximum when P_{IN} is at the null value and decreases when the input pressure P_{IN} to the converter either increases or decreases from the null value. The maximum conditioning-circuit output pressure corresponds to that oscillator circuit input pressure P_2 which causes the pulse frequency to be zero. The minimum output pressure from the conditioning circuit corresponds to the oscillator circuit input pressure, which causes the pulse frequency of the oscillator circuit to be the desired maximum value. To provide flat saturation characteristics, the minimum conditioning-circuit output pressure must not fall below this value.

The desired conditioning circuit input-output characteristics are shown graphically in figure 5. This curve was constructed by cross plotting the desired overall analog-to-pulse-frequency converter input-output characteristics (fig. 1) with experimentally determined, oscillator-circuit input-output characteristics. The experimentally determined oscillator characteristics are presented in the RESULTS AND DISCUSSION section.

The conditioning circuit consists of two proportional amplifiers. Amplifier A-4 in

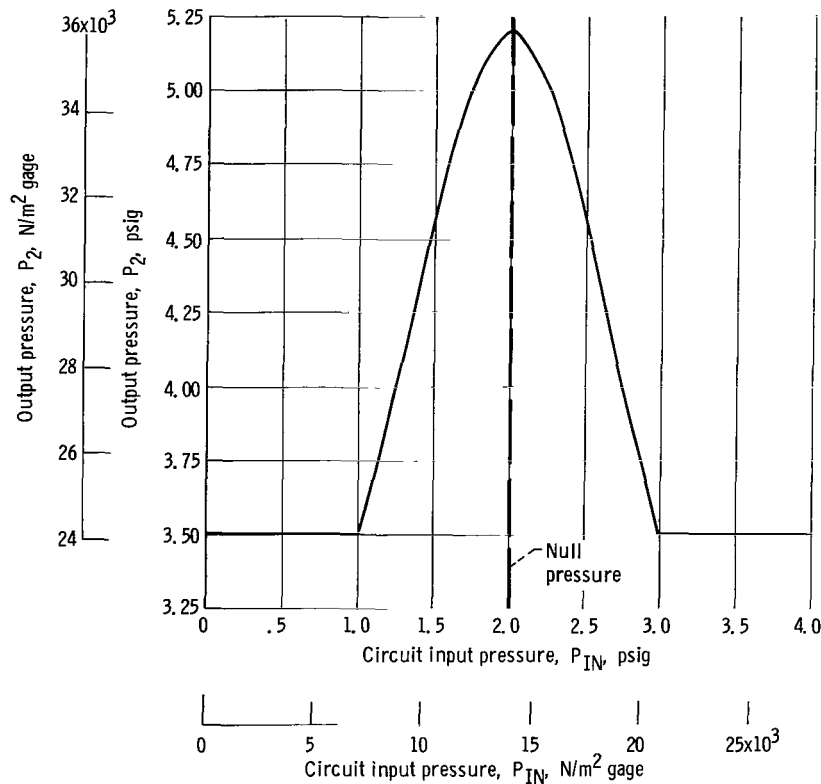


Figure 5. - Required input-output characteristics of conditioning circuit.

figure 3 is a center-output amplifier that is not available commercially. This amplifier will be described in the Breadboard Circuit section. An additional flow source is provided through valve V-1. This source maintains the output pressure of amplifier A-4 at the desired minimum pressure. Valve V-2 is used to set the null pressure at the desired value.

Output selector circuit. - The output selector circuit directs the oscillator output pulses to either the backward output port or the forward output port. If, as shown in figure 1, the converter input pressure P_{IN} is greater than the null pressure, the pulses appear at the forward pulse output port. If the input pressure P_{IN} is less than the null pressure, the pulses appear at the backward pulse output port.

Amplifier A-6 is a NOR-gate that serves to amplify the pulses produced by the oscillator circuit. The output of amplifier A-6 is applied to the supply port of bistable amplifier A-7. The pulses are directed toward either the forward pulse output port or the backward pulse output port depending upon which control port pressure of amplifier A-7 is greater. Proportional amplifier A-8, which provides the control input pressures to amplifier A-7, serves to increase the switching sensitivity of the selector circuit. Valve V-3 is set so that amplifier A-7 switches when P_{IN} equals the null pressure. NOR-gates A-9 and A-10 amplify the output pulse pressures.

Breadboard Circuit

A breadboard circuit of the analog-to-pulse-frequency converter was constructed of commercially available fluid jet amplifiers (except amplifier A-4). A photograph of the breadboard circuit is shown in figure 6. The two resistances, R_2 and R_3 , in the oscillator circuit were 0.039-inch-diameter (0.99×10^{-3} -m-diam) orifices, and volumes C_2 and C_3 were each 0.069 cubic inch (0.11×10^{-5} m³). This combination furnishes a calculated time constant of approximately 2 milliseconds. The method for calculating this time constant is given in appendix C.

Commercial amplifiers. - The commercial amplifiers are made of photoetched ceramic with barbed pressure fittings. The fittings were drilled out to accept 0.125-inch-outside-diameter (3.18×10^{-3} -m-o. d.) tubing which was used to interconnect components. This tubing had an inside diameter of 0.076 inch (1.9×10^{-3} m). Engineering and performance data on the commercial amplifiers are given in table I (p. 27).

Center-output amplifier. - The requirement for the center-output amplifier A-4 is that it produce an output signal which is a maximum when its control pressures are equal. As the differential control pressure varies from zero, the output pressure of the amplifier decreases. The amplifier which was developed to have these characteristics is shown in outline form in figure 7.

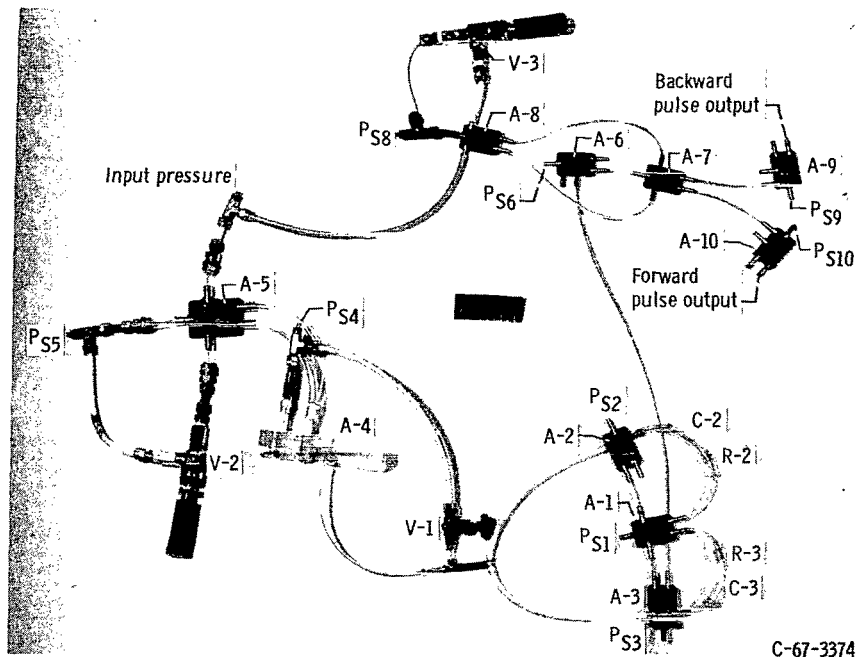
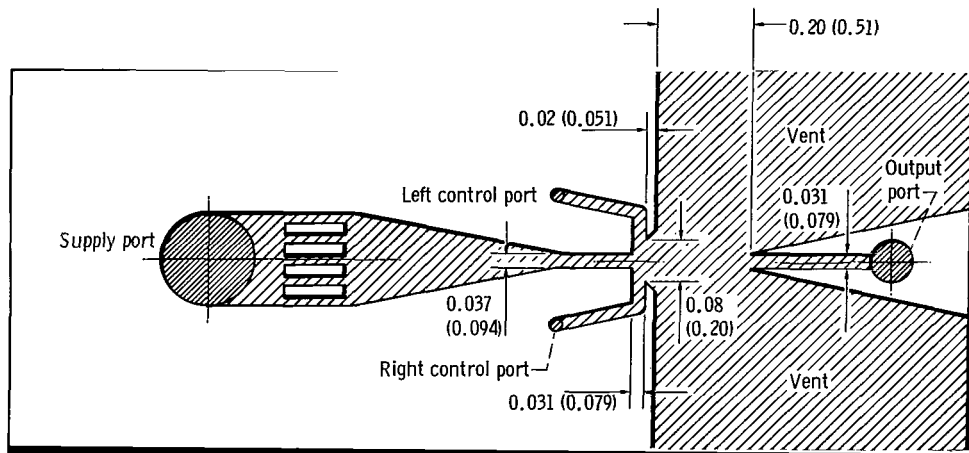


Figure 6. - Analog-to-pulse-frequency converter.

C-67-3374



CD-9528

Figure 7. - Outline of center-output proportional amplifier. Dimensions in inches (centimeters). Engraved depth (shaded area), 0.090 inch (0.25 cm).

In the conditioning circuit, as shown in figure 3, a differential pressure from the output of amplifier A-5 drives the center-output amplifier. However, for purposes of explaining the operation of the amplifier, consider the amplifier alone and assume the left control port is supplied with a constant bias pressure. This bias pressure deflects the power jet away from the output port when the pressure to the right control port is zero. As the right control port pressure is increased, the power jet is deflected towards the center output port to increase the output pressure. When the right control

port pressure equals the left control port pressure, the power jet is centered to create maximum output pressure. In the conditioning circuit this occurs when the input to amplifier A-5 is at the null pressure. As the right control port pressure is increased further, the power jet is deflected past the output port and the output pressure decreases. Thus, an input-output characteristic curve similar in shape to the curve of figure 5 is generated.

RESULTS AND DISCUSSION

Converter Steady-State Tests

The output pulse frequency of the breadboard analog-to-pulse-frequency converter is plotted in figure 8 as a function of input pressure P_{IN} . The output pulses were

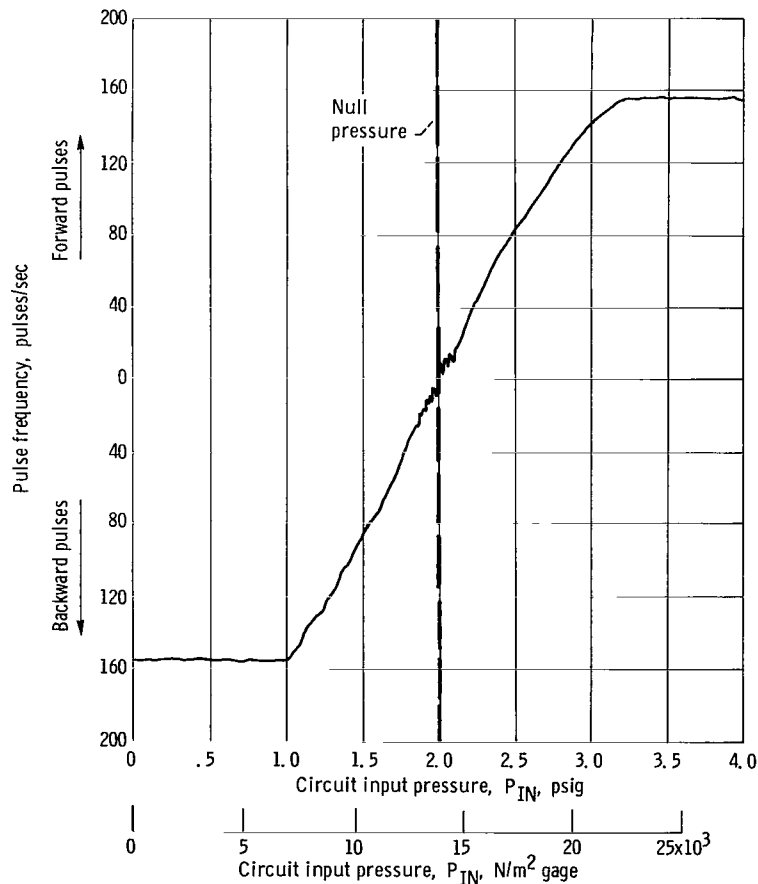


Figure 8. - Analog-to-pulse-frequency converter steady-state performance.

measured with a piezoelectric crystal pressure transducer and converted to a voltage by a frequency-to-voltage converter. The transducer was connected first to the forward pulse port and then to the backward pulse port in order to obtain the complete curve. The oscillations observed around zero frequency are caused primarily by the inability of the frequency-to-voltage converter to respond to low frequencies.

Oscillator-Circuit Response Tests

A test was conducted on the oscillator circuit to determine its response to a step change in input pressure P_2 . The input was stepped from 3.6 psig ($25 \times 10^3 \text{ N/m}^2$ gage) to 4.7 psig ($32 \times 10^3 \text{ N/m}^2$ gage) and back to 3.6 psig ($25 \times 10^3 \text{ N/m}^2$ gage), as shown in the upper oscilloscope trace of figure 9. The lower trace in this figure is of the oscillator output, which changes from 158 pulses per second to 71 pulses per second and back to 158 pulses per second. The output recovers from the input change within one output cycle.

Response tests were performed on the oscillator circuit only. Since the oscillator circuit was close coupled in the breadboard circuit, its configuration will not change significantly when made into an integrated circuit. However, this is not true of the conditioning circuit and the output selector circuit. It was necessary to use long interconnecting lines between components. The transmission delays of these lines cause poor total-system response. Poor response will not be present in an integrated circuit where

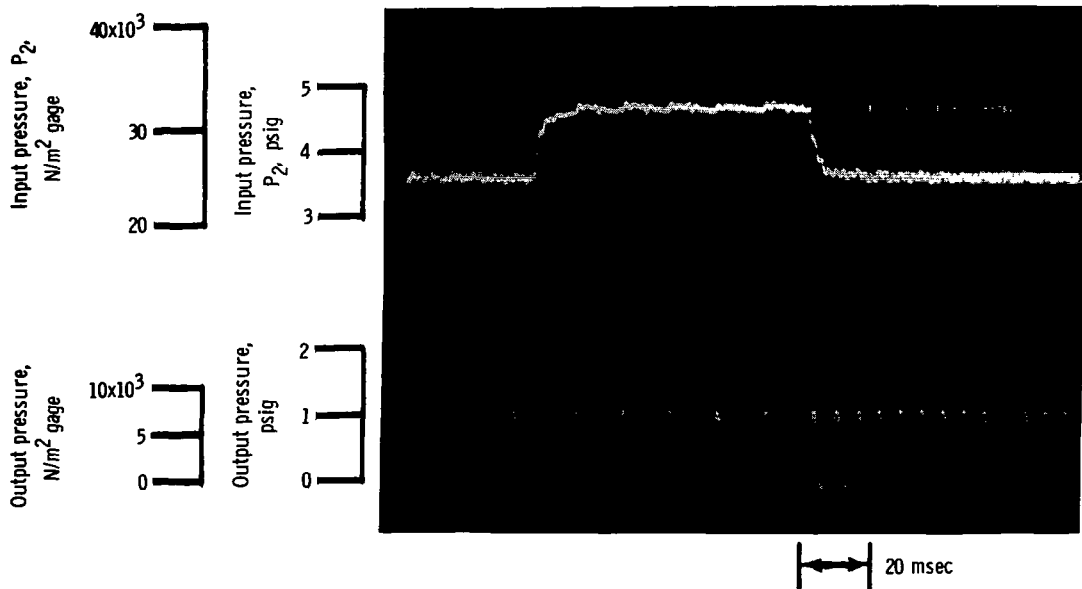


Figure 9. - Response of oscillator circuit to step change of input pressure.

all interconnecting passages are short. Experimental data on similar flueric components (ref. 4) show no appreciable change in amplitude ratio or appreciable phase lag up to frequencies of 100 hertz. The system response will be limited probably by interconnecting passages rather than by the flueric components.

Oscillator-Circuit Steady-State Tests

A test was run on the oscillator circuit to determine how its performance curve compared with the calculated curve presented previously in figure 4. The two curves are plotted in figure 10. The experimental curve differs from the calculated curve everywhere except at zero frequency. This deviation could be caused by an actual amplifier switching time of less than the 0.5 millisecond assumed in determining the calculated curve. For example, if the switching time were assumed to be 0.2 millisecond,

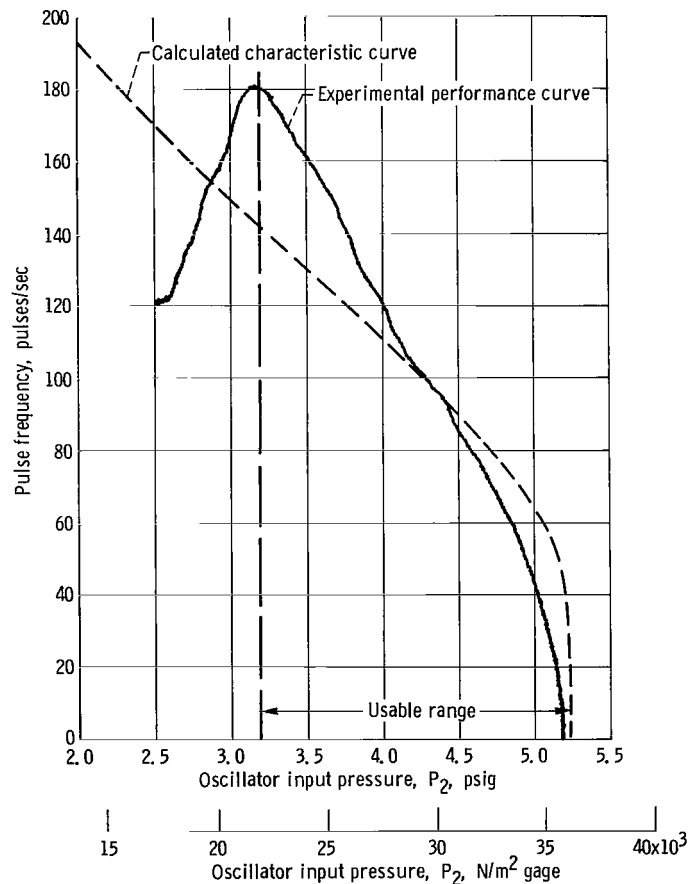
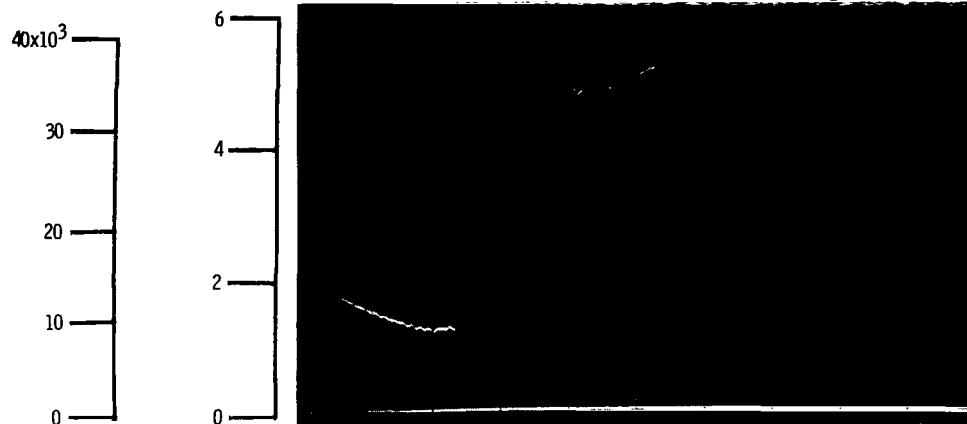
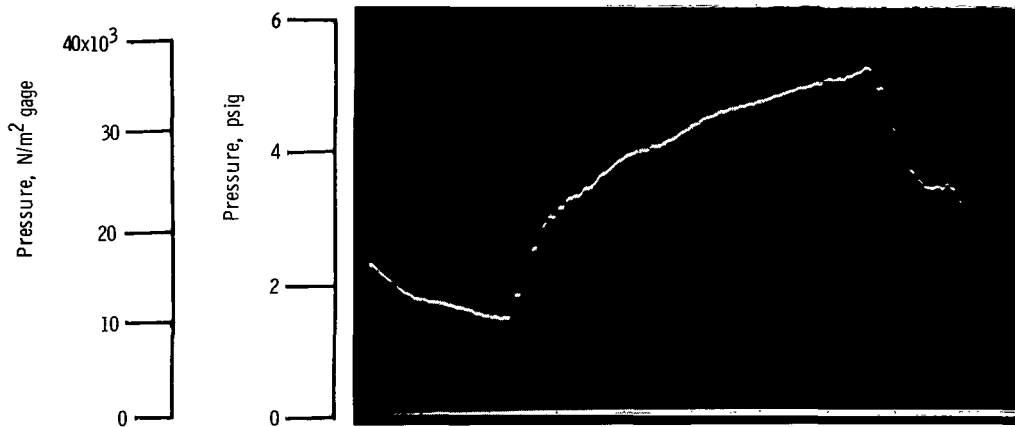


Figure 10. - Oscillator-circuit performance curve.



(a) Output of amplifier A-1.



(b) Input to amplifier A-2.



(c) Output of amplifier A-2.

Figure 11. - Waveforms of oscillator circuit.

the calculated frequency at an input pressure P_2 of 3.2 psig ($22 \times 10^3 \text{ N/m}^2$ gage) would be 170 pulses per second instead of 141 pulses per second. Also, it was assumed that the pressure wave at the inputs to amplifiers A-2 and A-3 is described by the equation for the response of a first-order system to a step input:

$$\frac{P}{P_{SS}} = 1 - e^{-t/RC}$$

Since pneumatic resistances and pneumatic capacitances are not linear, this equation is approximate and predicts accurately the switching pressures of amplifiers A-2 and A-3 at zero frequency only (see appendix C).

It should also be noted in figure 10 that the frequency decreases for pressures lower than about 3.2 psig ($22 \times 10^3 \text{ N/m}^2$ gage). This decrease is caused by interference between the input pulses on the control ports of amplifier A-1 at higher frequencies. Since this limitation occurs at frequencies higher than those for which the circuit was designed, it has no effect on the performance of the complete system. Appendix D describes this phenomenon in detail.

It has been shown that the oscillator frequency is affected by the C_1 and C_2 volume rise times. However, the output frequency is also affected by the switching time of the amplifiers and by the rise time of the output pulses from amplifiers A-2 and A-3. The switching time of the amplifiers is less than 0.5 millisecond. The output rise time of the pulses is made small by correctly matching the interconnection line impedance with the amplifier characteristics. The line sizes for the oscillator were determined by using the procedure outlined in reference 1.

Figure 11 shows the experimental waveforms for (a) the output of amplifier A-1, (b) the input to amplifier A-2, which is the volume C_2 pressure, and (c) the output of amplifier A-2.

Conditioning-Circuit Steady-State Tests

The output pressure P_2 of the breadboard conditioning circuit is plotted in figure 12 as a function of the circuit input pressure P_{IN} . The test was conducted with the conditioning-circuit output connected to the oscillator circuit. Note the agreement between the experimental curve and the desired curve taken from figure 5.

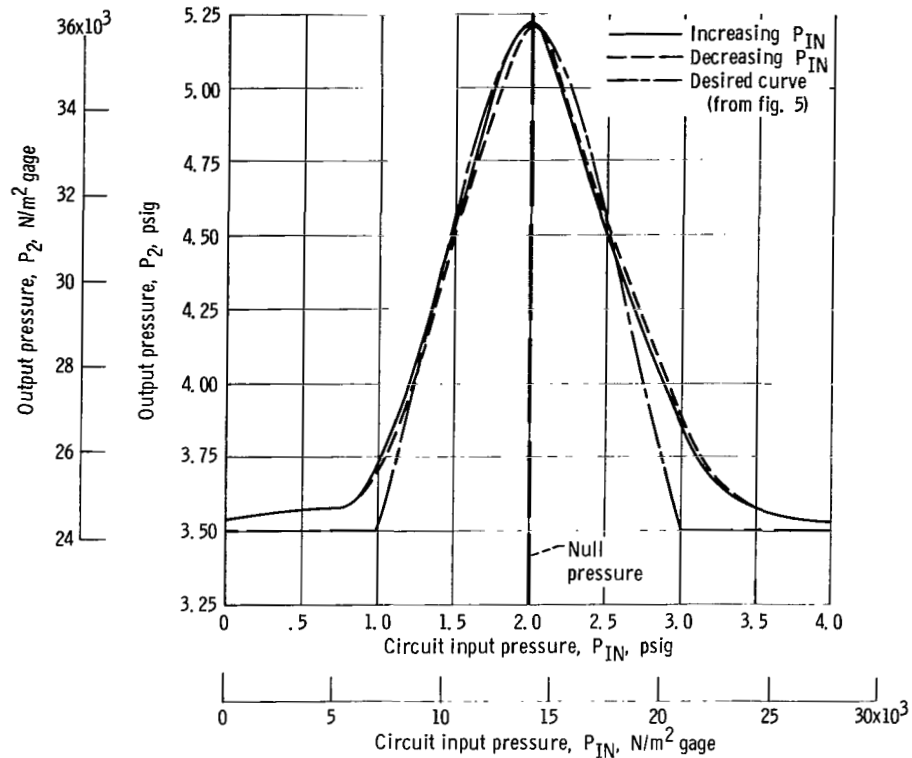


Figure 12. - Experimental input-output characteristics of conditioning circuit.

CONCLUSIONS

An analog-to-pulse-frequency converter was designed, and a breadboard of the converter circuit was built of commercial fluidic amplifiers.

The performance of the breadboard circuit satisfactorily meets the input signal conversion requirements of the actuator system described in appendix B. If the actuator system response is improved to more than 160 pulses per second, I believe that the analog-to-pulse-frequency converter circuit can be altered to operate at higher frequency by decreasing the time constant of the R_2C_2 and R_3C_3 portions of the oscillator circuit.

The step response tests show that the oscillator circuit can respond to a step change of input pressure within one output pulse. A close-coupled integrated circuit of the converter system should exhibit a response capability comparable to that of the oscillator circuit.

Lewis Research Center,
National Aeronautics and Space Administration,
Cleveland, Ohio, December 13, 1967,
122-29-03-04-22.

APPENDIX A

SYMBOLS

$A-1, A-2$ $\dots, A-10$	}	amplifier identification
$A, \bar{A}, B, \bar{B},$ C, \bar{C}, D, \bar{D}	}	bellows identification
C_2, C_3		volume identification
C		pneumatic capacitance, $\text{ft}^2 \frac{\text{lb mass}}{\text{lb force}} \left(\frac{\text{m}^2 \text{ kg}}{\text{N}} \right)$
e		Napierian base
f		frequency, Hz
k		ratio of specific heats
P		pressure, psig (N/m^2 gage)
P_F		amplifier forward switching pressure, psig (N/m^2 gage)
P_{IN}		circuit input pressure, psig (N/m^2 gage)
P_R		amplifier reverse switching pressure, psig (N/m^2 gage)
P_{SS}		maximum volume C_2 and C_3 pressure, psig (N/m^2 gage)
$P_{S1}, P_{S2},$ \dots, P_{S10}	}	amplifier supply pressures, psig (N/m^2 gage)
P_2		oscillator input pressure, psig (N/m^2 gage)
R		pneumatic resistance, $\frac{\text{lb force}/\text{in.}^2}{\text{lb mass}/\text{sec}} \left(\frac{\text{N}/\text{m}^2}{\text{kg}/\text{sec}} \right)$
R_c		amplifier A_2 and A_3 control port resistance, $\frac{\text{lb force}/\text{in.}^2}{\text{lb mass}/\text{sec}} \left(\frac{\text{N}/\text{m}^2}{\text{kg}/\text{sec}} \right)$
R_G		gas constant, $\frac{\text{ft}\cdot\text{lb force}}{(\text{lb mass})(^\circ\text{R})} \left(\frac{\text{J}}{(^{\circ}\text{K})(\text{mole})} \right)$
R_2, R_3		resistance identification

T	absolute temperature, $^{\circ}\text{R}$ ($^{\circ}\text{K}$)
t	time, sec
V	volume, ft^3 (m^3)
V-1, V-2, V-3	valve identification
τ_{F}	transit time for pressure wave to travel length of one feedback path, sec
τ_{L}	volume C_2 and C_3 pressure rise time, sec
τ_{RC}	time constant for R_2C_2 and R_3C_3 , sec
τ_{SW}	amplifier switching time, sec
τ_{T}	total loop transit time for both feedback paths, sec

APPENDIX B

ACTUATOR SYSTEM DESCRIPTION

Actuator

A pneumatic stepping actuator (fig. 13) was developed under a NASA Lewis Research Center contract for positioning nuclear rocket engine control drums. This development work is described in reference 5.

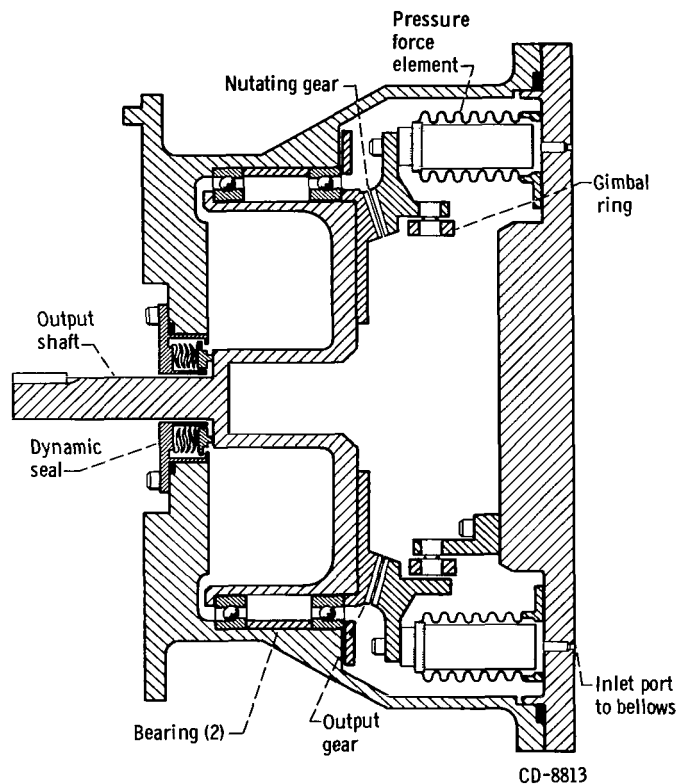


Figure 13. - Cross-section of pneumatic stepping actuator.

A simplified schematic of the actuator is shown in figure 14. The two basic parts of the motor are an output gear, which is free to rotate only, and a nutating gear, which is free to nutate, or wobble, only. The nutating gear is actuated by eight bellows located around the periphery of the gear. The gear is tilted and forced into contact with the output gear by always keeping four adjacent bellows pressurized. The nutating gear is driven by advancing the pressurization pattern around the eight bellows as shown in figure 15. The output gear has 180 teeth, and the nutating gear has 181 teeth. As the nu-

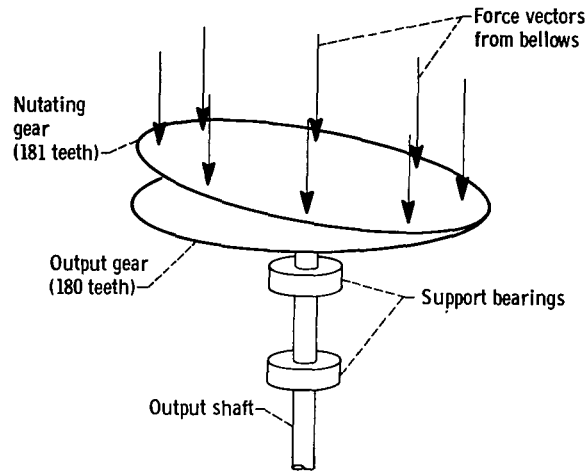
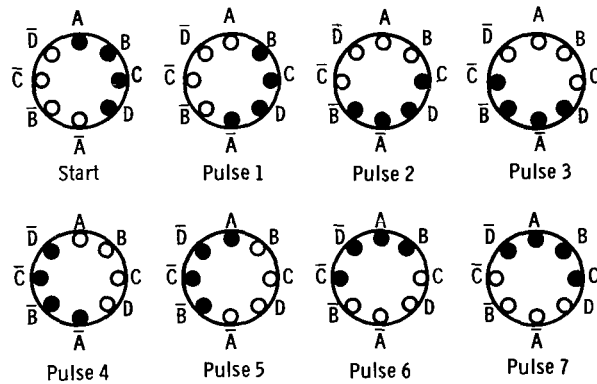
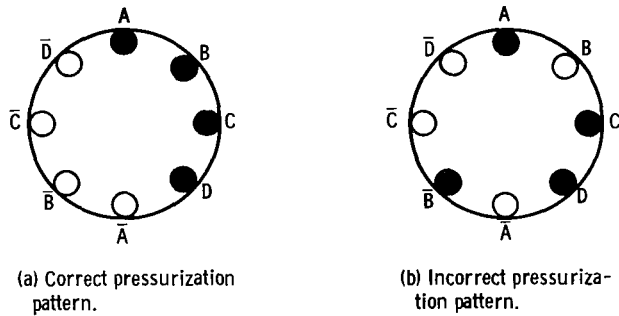


Figure 14. - Schematic of pneumatic stepping actuator.



(c) Sequencing of pressure pattern by forward-counting input pulses.

Figure 15. - Bellows pressurization patterns.

tating gear moves through one nutating cycle, the output gear must advance one tooth or 2° of rotation. Since for one cycle the pressurization pattern moves through eight bellows, each step causes the output gear to advance 0.25° .

Logic Circuit

The pressurization pattern to the motor is generated by a fluidic logic circuit developed at the NASA Lewis Research Center. A complete description of this circuit is presented in reference 1.

The logic circuit shown in block diagram form in figure 16 consists of four subcircuits: two pulse conditioning circuits, a counting circuit, and a power amplifier circuit.

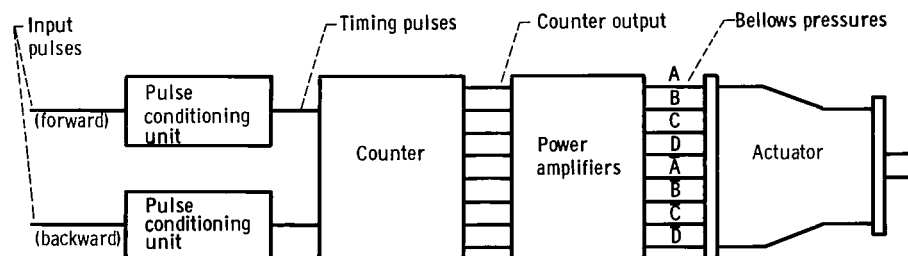


Figure 16. - Block diagram of actuator system.

Pulse conditioning circuit. - The purpose of the pulse conditioning circuit is to receive the input pulses and convert them into pulses of suitable shape, height, and width for use as command pulses to the counting circuit. One pulse conditioning circuit is required for forward command pulses and one for backward command pulses.

Counting circuit. - The counting circuit furnishes the proper bellows pressurization pattern to the stepping motor. The pattern is stored by the counter and is shifted forward or backward when command pulses are received by the logic circuit.

Power amplifiers. - The output amplifiers of the counting circuit do not have sufficient output flow capacity to drive the stepping motor bellows. Four supersonic bistable fluid jet power amplifiers (developed at the NASA Lewis Research Center) were used between the counting circuit and actuator to provide sufficient pressures and flows. This amplifier is described in reference 1.

APPENDIX C

OSCILLATOR CALCULATED FREQUENCY

This appendix presents the procedure used to determine the curve, shown in figure 4, of the oscillator-circuit calculated frequency as a function of input pressure. Included herein are the assumptions used to determine the curve and the methods used in determining these assumptions.

The oscillator frequency is determined by the following equation:

$$f = \frac{1}{\tau_T} \quad (C1)$$

where τ_T is the total loop transit time for both feedback paths. The components of τ_T are shown in the equation

$$\tau_T = 2\tau_F + 4\tau_{SW} + 2\tau_L \quad (C2)$$

The time required for a pressure wave to travel the length of one feedback path is τ_F . Since the speed of sound at room temperature is approximately 13 inches (3.3×10^{-1} m) per millisecond, and the loop length is 6 inches (1.5×10^{-1} m), τ_F is approximately 0.5 millisecond. The switching time τ_{SW} for each amplifier was less than 0.5 millisecond, and this was used for these calculations. The time required for the pressure in volumes C_2 and C_3 to rise to the switching pressure of amplifiers A-2 and A-3 is τ_L .

In determining τ_L it was assumed that the pressure rise in volumes C_2 and C_3 is described by the equation for the response of a first-order system to a step input:

$$\frac{P}{P_{SS}} = 1 - e^{-t/\tau_{RC}} \quad (C3)$$

where P is pressure, P_{SS} is the maximum volume pressure (experimentally determined as 6.0 psig (41×10^3 N/m² gage)), t is time, and τ_{RC} is the time constant for the R-C combinations R_2C_2 and R_3C_3 .

To determine the time delay τ_L , equation (C3) can be rewritten as follows:

$$P_F = \left(1 - e^{-\tau_L/\tau_{RC}}\right) P_{SS} \quad (C4)$$

where P_F is the pressure required at volume C_2 or C_3 to switch amplifiers A-2 and A-3. This pressure is a function of the pressure on the opposite control port P_2 and of the supply pressures P_{S2} and P_{S3} of amplifiers A-2 and A-3. For the amplifiers used in the oscillator circuit

$$P_F = 1.06 P_2 + 0.08 P_{S2} \quad (C5)$$

This equation was obtained experimentally from a bistable amplifier similar to those used in the oscillator circuit.

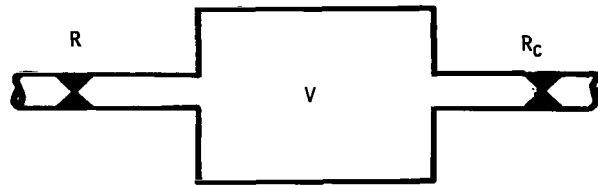


Figure 17. - Simple pneumatic resistance-capacitance circuit.

The RC time constant τ_{RC} was determined for the simplified system shown in figure 17.

$$\tau_{RC} = \frac{RR_c}{R + R_c} \mathcal{C} \quad (C6)$$

The capacitance \mathcal{C} for volume V was determined by the equation

$$\mathcal{C} = \frac{V}{kR_G T} \text{ (assumed adiabatic expansion)} \quad (C7)$$

where V is volume, k is the ratio of specific heats, R_G is the gas constant, and T is absolute temperature.

The upstream orifice resistance R was determined from a theoretical curve of flow as a function of downstream pressure through the R_2 and R_3 orifices. The up-

stream pressure was assumed to be constant at an experimentally determined value of 6.1 psig ($42 \times 10^3 \text{ N/m}^2$ gage). The linearized value of resistance R was chosen as the reciprocal of the slope of the curve at a downstream pressure equal to $P_{SS}/2$. This value was determined to be $1.8 \times 10^4 \text{ (lb force/in.}^2\text{)/(lb mass/sec)}$ ($2.7 \times 10^8 \text{ (N/m}^2\text{)/(kg/sec)}$).

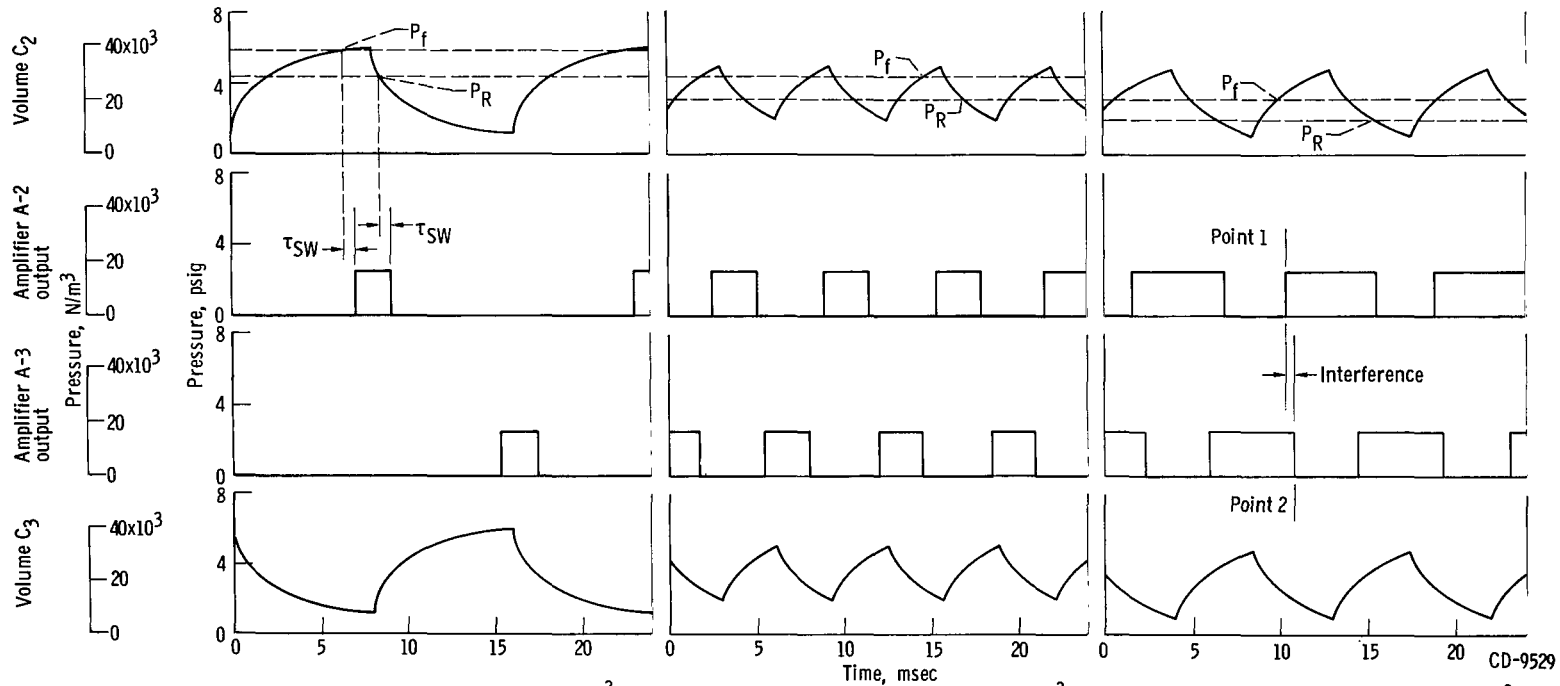
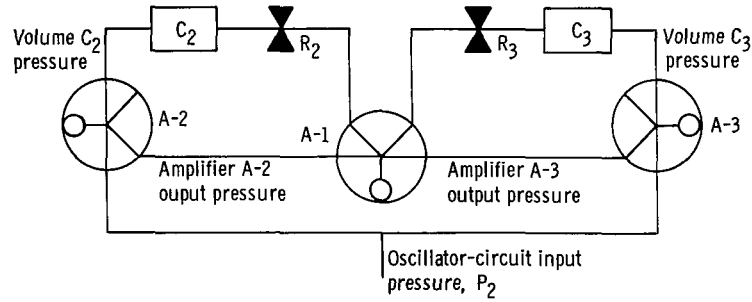
The control port resistance R_c was determined from an experimental plot of the control port characteristics of a bistable amplifier similar to those used in the oscillator circuit. The value of R_c was chosen as the slope of the curve of control port pressure as a function of control port flow at a control port pressure of $P_{SS}/2$. The pressure in the opposite control port P_2 was also assumed to be $P_{SS}/2$. From appendix C of reference 1, resistance R_c was determined to be $3.8 \times 10^4 \text{ (lb force/in.}^2\text{)/(lb mass/sec)}$ ($5.8 \times 10^8 \text{ (N/m}^2\text{)/(kg/sec)}$). By using these values of resistances and calculating a capacitance C of $0.1 \times 10^{-8} \text{ ft}^2 \text{ (lb mass/lb force)}$ ($0.95 \times 10^{-11} \text{ m}^2 \text{ (kg/N)}$) based on a volume of 0.069 cubic inch ($0.11 \times 10^{-5} \text{ m}^3$), τ_{RC} was calculated to be approximately 0.002 second.

APPENDIX D

OSCILLATOR-CIRCUIT MAXIMUM FREQUENCY LIMITATION

Figure 10 shows that when the oscillator-circuit input pressure P_2 is less than about 3.2 psig (22×10^3 N/m² gage) the experimental oscillator frequency decreases. This oscillator-circuit frequency limitation is caused by interference between the input pulses on the control ports of amplifier A-1. This can be seen by following the pulse sequence shown in figure 18. Figure 18(a) shows the pulse sequence when the oscillator circuit input pressure P_2 is set at 4.8 psig (33×10^3 N/m² gage), which results in a pulse frequency of 63 pulses per second. The volume C_2 pressure rise (fig. 18) appears at the control port of amplifier A-2. The pressure at which amplifier A-2 switches, P_F , depends on its opposite control port pressure P_2 and can be determined from figure 19. Figure 19 is a plot of the experimentally determined amplifier forward switching pressures, P_F , and reverse switching pressures, P_R , as functions of the pressure P_2 at the opposite control port. It should be noted that the volume C_2 pressure must be greater than the oscillator input pressure P_2 before amplifier A-2 will switch to the control port of amplifier A-1. Also, volume C_2 pressure must decrease to a value less than the oscillator input pressure P_2 before amplifier A-2 will switch from the control port of amplifier A-1. It is seen from figure 18 that the forward switching pressure P_F and reverse switching pressure P_R of amplifier A-2 determine the width of the output pulse of amplifier A-2 for any given input pressure P_2 and volume pressure waveform.

As the oscillator input pressure P_2 decreases to 3.5 psig (24×10^3 N/m² gage), as shown in figure 18(b), the time between the forward switching pressure P_F and reverse switching pressures P_R has increased. This increase in time causes the width of the output pulse of amplifier A-2 to increase. As the oscillator input pressure P_2 is decreased still further, the point is reached where the pulse width becomes equal to the time between pulses. At a still lower oscillator input pressure P_2 the output pulses from amplifier A-2 are still on the control port of amplifier A-1 when the output pulse from amplifier A-3 is applied to the opposite control port of amplifier A-1. Amplifier A-1 cannot switch to resistance R_2 until the output pulse of amplifier A-2 vanishes.



(a) Oscillator input pressure, 4.8 psig (33×10^3 N/m² gage). Pulse frequency, 63 pulses per second.

(b) Oscillator input pressure, 3.5 psig (24×10^3 N/m² gage). Pulse frequency, 161 pulses per second.

(c) Oscillator input pressure, 2.5 psig (17×10^3 N/m² gage). Pulse frequency, 120 pulses per second.

Figure 18. - Oscillator pulse sequence for various oscillator input pressures.

CD-9529

Thus, the maximum frequency is limited. As the oscillator circuit input pressure is decreased still further, the interference between the output pulses from amplifiers A-2 and A-3 becomes greater and the output pulse frequency decreases. This is shown in figure 18(c), where the oscillator input pressure P_2 is 2.5 psig ($17 \times 10^3 \text{ N/m}^2$ gage). Note that when amplifier A-2 switches to amplifier A-1 (shown as point 1 in fig. 18(c)), amplifier A-3 is still switched to the opposite control port of amplifier A-1. Amplifier A-1 cannot switch into resistance R_3 until the pulse from amplifier A-3 switches from the control port of amplifier A-1 (shown as point 2 in fig. 18(c)).

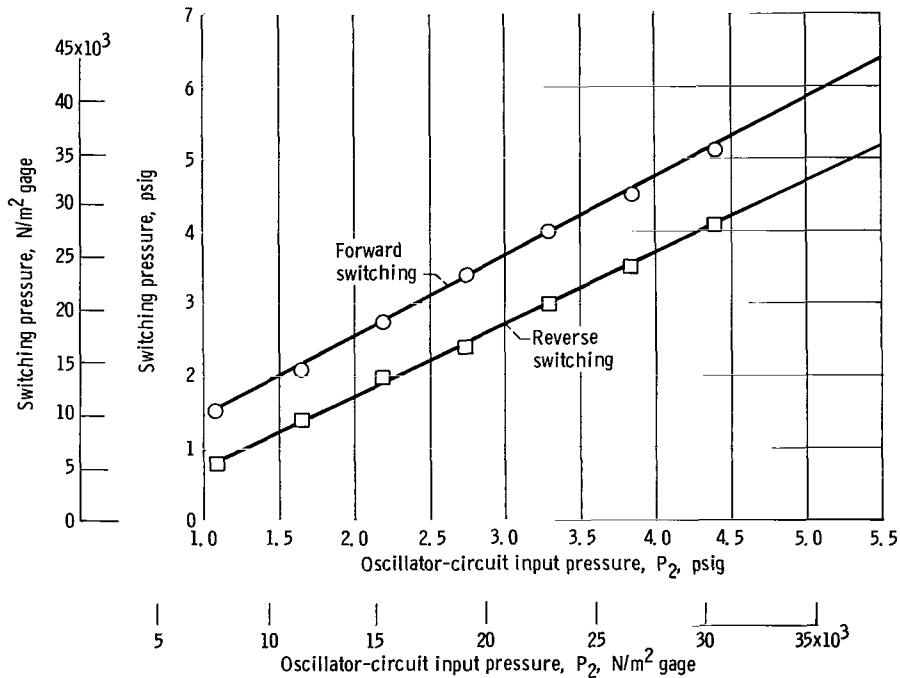


Figure 19. - Switching characteristics of amplifiers A-2 and A-3.

REFERENCES

1. Griffin, William S.: Breadboard Fluoric-Controlled Pneumatic Motor System. NASA TN D-4495, 1968.
2. Kirshner, J. M.; and Campagnuolo, C. J.: A Temperature-Insensitive Pneumatic Oscillator and a Pressure-Controlled Pneumatic Oscillator. Proceedings of the Fluid Amplification Symposium. Vol. II. Harry Diamond Labs., 1965, pp. 5-19. (Available from DDC as AD-623456.)
3. Manion, F. M.: Development of a Pressure Controlled Oscillator for FM Systems. Proceedings of the Fluid Amplification Symposium. Vol. II. Harry Diamond Labs., 1965, pp. 21-45. (Available from DDC as AD-623456.)
4. Brown, F. T.: Stability and Response of Fluid Amplifiers and Fluidic Systems. Rep. No. DSR5169-3 (NASA CR-72192), Massachusetts Inst. Tech., Nov. 1967.
5. Howland, G. R.: Pneumatic Nutator Actuator Motor. Rep. No. BPAD-863-16719R (NASA CR-54788), Bendix Corp., Oct. 17, 1965.

**TABLE I - PERFORMANCE, ENGINEERING DATA, AND SUPPLY PRESSURES FOR
FLUERIC AMPLIFIERS USED IN BREADBOARD CIRCUIT**

Amplifier	Type of amplifier	Size of power nozzle		Size of control nozzle		Supply pressure		Maximum pressure recovery, percent of supply pressure
		in.	cm	in.	cm	psig	N/m ² gage	
A-1	Wall attachment; bistable	0.010×0.040	0.025×0.100	0.010×0.040	0.025×0.100	20.0	138×10 ³	33
A-2	Wall attachment; bistable	.010×0.040	.025×0.100	.010×0.040	.025×0.100	5.5	38×10 ³	33
A-3	Wall attachment; bistable	.010×0.040	.025×0.100	.010×0.040	.025×0.100	5.5	38×10 ³	33
A-4	Beam deflection; proportional; center output	.037×0.090	.094×0.229	.031×0.090	.079×0.229	5.6	39×10 ³	(a)
A-5	Beam deflection; proportional	.020×0.050	.051×0.127	.030×0.050	.076×0.127	15.0	103×10 ³	40
A-6	Wall attachment; OR-NOR gate	.010×0.040	.025×0.100	-----	-----	20.0	138×10 ³	35
A-7	Wall attachment; bistable	.010×0.040	.025×0.100	.010×0.040	.025×0.100	(b)	-----	33
A-8	Beam deflection; proportional	.010×0.025	.025×0.064	.015×0.025	.038×0.064	10.0	69×10 ³	55
A-9	Wall attachment; OR-NOR gate	.010×0.040	.025×0.100	-----	-----	10.0	69×10 ³	35
A-10	Wall attachment; OR-NOR gate	.010×0.040	.025×0.100	-----	-----	10.0	69×10 ³	35

^aNot measured.

^bNo supply.

